BL-6A/2021G040

Effects of Layer Deformation on Mechanical Properties of Glassy Smectic Liquid Crystal Polymer Fibers

Katsuki Kawahara, Ryoji Suzuki, and Masatoshi Tokita*
Department of Chemical Science and Engineering, Tokyo Institute of Technology,
Ookayama, Meguro, Tokyo 152-8550, Japan

1 Introduction

Stacked layers are one of the typical molecular assemblies found in solid polymers, including semicrystalline polymers and block copolymers (BCPs). When stacked layers are elongated along the layer normal direction, the layers undulate and form chevrons by bending at limited sites to avoid the increase in spacing.[1–3] These structural changes are associated with stress responses, such as stress yielding. In these studies, the layers were flat and large. Once deformed layers have rarely been examined for deformation and stress response under another sample deformation.

In this study,[4] we examine the effects of layer deformation on the stress response for a smectic liquid crystal (LC) composed of a main-chain BB-5(3-Me) polyester comprising biphenyl moieties connected with alkyl spacers via ester linkages (Fig. 1).[5–7] Fibrous specimens prepared by stretching the isotropic melt had layers stacked along the fiber axis. Elongating this fiber in the LC state deformed the layers, yielding fibers with two types of layer morphologies: layers stacked along a direction tilted from the fiber axis and layers divided and stacked along the fiber axis. Fibers with different layer deformation types differed in their stress response upon tensile deformation in a glassy state, as determined using synchrotron-radiation X-ray diffraction (XRD). The results demonstrate that dividing the layers significantly increased the values of Young's modulus and yield stress of the fiber, respectively, by three and 2.5 times. This agrees with strengthening layer-structured polymeric materials by dividing the layers, which was recently reported for a lamellar block copolymer and a semicrystalline polymer.[8,9] This study will lead to the developing of a new method for strengthening polymer solids other than those with polymer chain or crystal orientation. However, other layer-structured materials, such as metallic alloys and MAX-phase ceramics, have been strengthened by kinking the layers.[10,11]

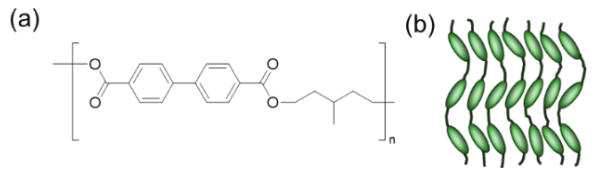

Fig. 1. (a) Chemical structure of a BB-5(3-Me) polyester and (b) smectic LC structure formed by the polyester. Mesogenic biphenyl moieties represented with filled ellipsoids form layers by segregating from the alkyl spacers represented with the sold lines.

2 Experiment

Materials: The BB-5(3-Me) polyester was prepared by the melt condensation of dimethyl 4,4′-biphenyl dicarboxylate and 3-methyl-1,5-pentanediol.[5,6] The number-average molecular weight (M_n = 48 kg mol^{-1}) and the polydispersity index (PDI = 1.7) were determined by size-exclusion chromatography (SEC) calibrated with polystyrene standards. This polyester had a glass transition temperature T_g = 33 °C and an isotropization temperature T_i = 153 °C, measured by differential scanning calorimetry (DSC) at a heating rate of 10 °C min^{-1}.

Methods: Synchrotron-radiation XRD measurements were performed at the BL-6A beamline at Photon Factory, Tsukuba, Japan, using a Dectris Pilatus3 1M detector.[12] The X-ray radiation wavelength (λ_X) and the sample-to-detector distance were 0.15 nm and 0.25 m, respectively. A film sample at a predetermined temperature was continuously stretched using a Linkam TST350 tensile stage at a crosshead speed of 1.3 μm s^{-1} (nominal strain rate: 5% min^{-1}). The test sample length and cross-sectional dimensions were 1.5 mm and 0.4–0.6 × 0.2–0.4 mm^2, respectively. The XRD patterns were recorded at an exposure time of 30 s.

3 Results and Discussion

3.1. Smectic layer deformations

Stretching the fiber in the LC state deformed the smectic layers. This enabled us to prepare three types of glassy smectic LC fibers with deformed layers: fibers A, B, and C in order of increasing ε. Fiber A was the nondeformed fiber (ε = 0%) with smectic layers stacked along the fiber axis (Fig. 2a). This fiber displayed the layer reflection on the meridional line, indicating that the smectic layers were stacked along the fiber axis.

Fiber B, prepared by elongating the fiber up to ε = 30% at a strain rate of 1.25% min^{-1}, exhibited smectic layer reflection with intensity maxima at off-meridional positions (Fig. 2b). These intensity maxima indicated that the layer stacking direction was tilted from the fiber axis. This four-point reflection is usually associated with chevrons comprising layers periodically bent along the layers.[2,3,8,13,14] However, such periodic layer bending was not detected by Raman spectroscopy and polarizing microscopy.[4] We speculate that the tilted layers in fiber B alternated the layer stacking direction through the thickness direction of the fiber with a rectangular cross section. Besides the four-point reflection, the fiber left a reflection intensity on the meridian.

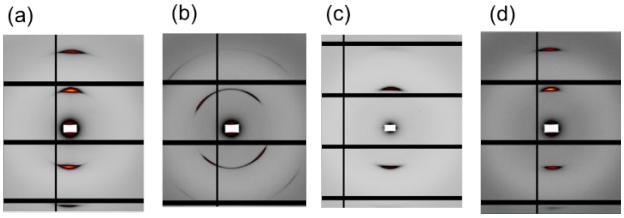

Fig. 2. XRD patterns measured for fibers (a) A, (b) B, (c) C, and (d) D at 25 °C. The fiber axis is vertical.

Fiber C, prepared by elongating the fiber up to ε = 300% at a rate of 5% min^{-1}, displayed the layer reflection on the meridian (Fig. 2c). This reflection was elongated in the horizontal direction parallel to the layers, indicating that the layers were divided and shortened.[15]

The divided layers recovered the layer length upon annealing fiber C at an LC temperature of 110 °C for 12 h. This annealed fiber, designated as fiber D, showed an XRD pattern that resembled that of fiber A (compare Fig. 2d to 2a), indicating that fiber D comprised long (or large-area) smectic layers like fiber A.

3.2. Stress Response of Fibrous Glassy Smectic LC Fibers with Predeformed Layers

The four types of BB-5(3-Me) fibers were examined for the stress response upon elongation in a glassy LC state at 25 °C. These fibers had rectangular cross sections. The cross-sectional dimensions of fibers A and B were 0.6 mm in width and 0.4 mm in thickness, and those of fibers C and D were 0.4 mm in width and 0.2 mm in thickness.

These fibers displayed different σ–ε curves (Fig. 3). These σ–ε curves allowed us to determine the values of Young's modulus (E), yield stress and strain (σ_y and ε_y), and strain at fiber break (ε_b) as follows. Fiber A with long layers stacked along the fiber axis showed E = 0.33 GPa and σ_y = 33 MPa at ε_y = 27% and broke at ε_b = 30%. Fiber B comprising layers tilted from the fiber axis showed E = 0.38 GPa and σ_y = 20 MP at ε_y = 23%. This fiber showed a long plateau on the σ–ε curve and increased σ slightly at ε = 200%, which was sustained up to the ε of the apparatus limit (300%). Fiber C with divided layers showed the highest E = 0.97 GPa and σ_y = 82 MPa among the four types of fibers, which were 3 and 2.5 times greater than those of fiber A. Fiber D showed two times greater E than fiber A and a similar σ_y to that of fiber A. Therefore, although the fibers were spun from the same polymer, they exhibited significantly different σ-ε curves at the same temperature and strain rate.

These differences in the σ–ε curves can be associated with different layer structures. Tilted layers make the fiber ductile as in fiber B. Divided layers increase E and σ_y, as shown for fiber C. This mechanical strengthening is associated with smaller layer dimensions. Annealing fiber C in the LC state recovered layer dimensions to be comparable to those in fiber A and decreased σ_y, as measured for fiber D. Consequently, the glassy smectic LC fiber, which is fragile in tensile deformation along the layer stacking direction, is effectively strengthened by dividing the layers and made more ductile by tilting the layers.

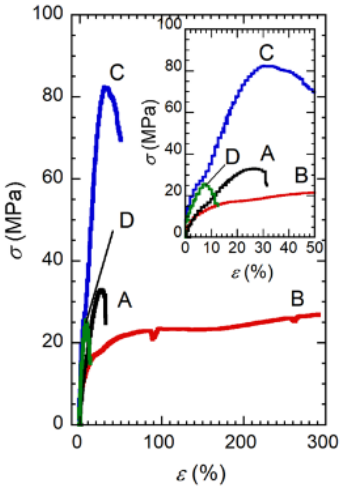

Fig. 3. σ–ε curves measured for fibers A, B, C, and D at 25 °C at a strain rate of 5% min^{-1}. The part at smaller ε is enlarged and shown in the inset.

3.3. Deformation of Layers in Glassy Smectic LC Fibers

The smectic layer deformation and stress response of the fibers were examined by measuring their synchrotron-radiation XRD patterns simultaneously with σ–ε curves. The patterns demonstrate that the predeformations of smectic layers affected the structural deformation as well as the stress response.

The tensile deformation of fiber A increased the layer spacing with increasing σ. The XRD patterns showed that the fiber elongation shifted the layer reflection toward smaller diffraction angles as ε increased (**Fig. 4**a–d). When the fiber broke, the reflection recovered its position (Fig. 4e). Thus, the increase in the layer spacing was proportional to σ (Fig. 4f), indicating that the layer dilation stored the mechanical energy of the tensile deformation.

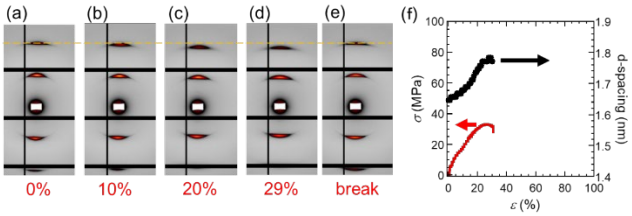

Fig. 4. (a–e) XRD patterns measured for fiber A elongated at 25 °C at the strains indicated below each panel. The fiber axis is vertical. The horizontal dashed line is shown to compare the position of the second-order layer reflection with that of the undeformed fiber. (f) Smectic layer spacings determined from the XRD patterns (black circles) and the measured strain (red curve), plotted against the fiber strain.

Fiber B comprised layers tilted at a larger angle with increasing ε (Fig. 5a–e). This fiber displayed layer reflection with four intensity maxima at the positions away from the meridional line. As ε increased, these maxima shifted away from the meridional line toward larger diffraction angles, decreasing the d-spacing (circular marks in Fig. 5f). This layer deformation maintained the polymer chain axis direction at 30° from the fiber axis, as

confirmed by Raman spectroscopy. The layer tilting, which decreased the d-spacing, is associated with sliding polymer chains along the chain axis. This polymer chain sliding disrupts the smectic layers composed of biphenyl moieties connected via aliphatic spacers; as a result, the layer reflection disappears. In addition, chain sliding is associated with the stress plateau at $\varepsilon > 50\%$, making the fiber ductile.

Besides, fiber B displayed a layer reflection intensity on the meridional line. This meridional reflection increased the d-spacing with increasing ε up to 50% (triangle marks in Fig. 5f). The layer spacing became constant as the increase in σ decreased at $\varepsilon > 50\%$.

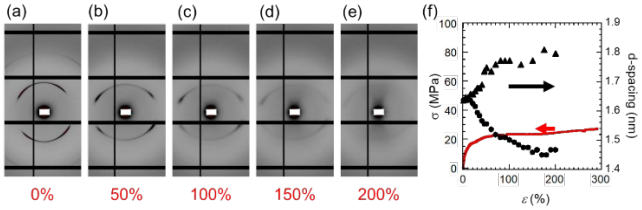

Fig. 5. (a-e) XRD patterns measured for fiber B stretched at 25 °C at the strains indicated below each panel. The fiber axis is vertical. (f) Smectic layer spacings determined from the XRD patterns (black marks) and the measured stress (red curve), plotted against the fiber strain. Two spacings were determined from the reflections on the meridional line (triangles) and from the off-meridional line intensity maximum (circles) on the patterns.

In case of fiber C, the spacing of short layers increased with the increasing ε. The XRD patterns include the layer reflection elongated in the horizontal direction (Fig. 6a–e). The diffraction angle of the layer reflection decreased as σ increased, demonstrating that tensile deformation influenced the layer spacing. The increase in layer spacing is comparable to that observed for the elongated fiber A (Fig. 6f). The layer spacing at $\varepsilon = 20\%$ measured for fiber C was 1.77 nm, similar to that obtained for fiber A (1.75 nm). Further, at the same ε, fiber C had σ = 68 MPa, 2.3 times greater than that obtained for fiber A (30 MPa).

This greater σ for fiber C is ascribed to the progress of layer division. As ε increased, fiber C displayed wider layer reflection along the horizontal direction, indicating that fiber C, with divided smectic layers at the unloaded state, further divided the layers upon tensile deformation. The reflection intensities along the horizontal line were evaluated, and the half width at half maximum (HWHM) values are plotted against ε (Fig. 6g). The HWHM increased with increasing σ. The HWHM increased more steeply at $\varepsilon > 20\%$, which seems to correspond to the steeper increase in σ at $\varepsilon > 10\%$. The division of smectic layers can dissipate the mechanical energy applied by tensile deformation, allowing fiber C to display greater E and σ_y than fiber A when considering the same layer dilation.

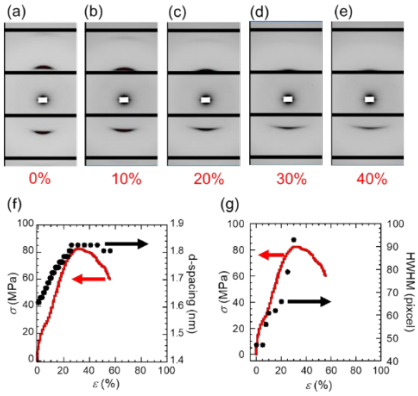

Fig. 6. (a–e) XRD patterns measured for fiber C elongated at 25 °C at the strains indicated below each panel. The fiber axis is vertical. (f) Smectic layer spacings obtained from the XRD patterns and (g) half width at half maximum (HWHM) values of the smectic layer reflection intensities measured from the XRD patterns along the horizontal direction plotted against the fiber strain. In (f) and (g), the stress values simultaneously measured with the XRD patterns are also shown (red curve).

Fiber D had long layers stacked along the fiber axis and displayed an XRD pattern similar to that measured for fiber A (compare Fig. 7a with Fig. 4a). The tensile deformation of the fiber with ε up to 4.5% shifted the layer reflection at a smaller angle (Fig. 7b–d). Then, at $\varepsilon = 10\%$, which was over the yielding point, the layer reflection appeared at a greater diffraction angle than that measured at $\varepsilon = 4.5\%$ (Fig. 7e). Thus, the increase in the layer spacing was proportional to σ, as for fibers A and C.

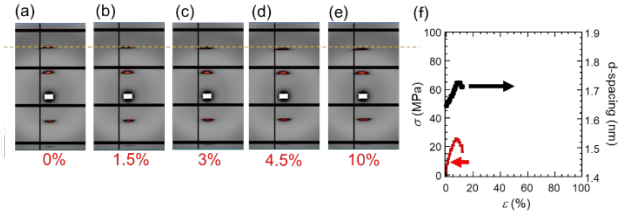

Fig. 7. (a–e) XRD patterns measured for fiber D elongated at 25 °C at the strains indicated below each panel. The fiber axis is vertical. The horizontal dashed line is shown to compare the position of the second-order layer reflection with that of the undeformed fiber. (f) Smectic layer spacings determined from the XRD patterns (black circles) and the measured strain (red curve), plotted against the fiber strain.

Glassy smectic LC fibers with the layer stacked along the fiber axis improve the ductility and toughness by tilting and dividing the layers, respectively. The high σ_y value of fiber C is certainly due to the divided layers. Fiber D, prepared by annealing fiber C in the LC state, recovered long layers and decreased σ_y to 25 MPa, comparable to that measured for fiber A. Fiber C under tensile deformation increased the smectic layer spacing as much as in fiber A, whereas the layers were more divided to dissipate mechanical energy, allowing the fiber to bore more significant stress than fiber A.

Acknowledgement

4,4′-dimethyl biphenyldicarboxylate was kindly supplied by Ihara-Nikkei Chemical Industry Co. Ltd. This study was supported by JSPS KAKENHI for Scientific Research on Innovative Areas "MFS Materials Science (Grant Number JP21H00095)".

References

[1] M. Krumova, S. Henning, and G.H. Michler, *Philos. Mag.*, **86**, 1689–1712 (2006).
[2] Y. Cohen, R.J. Albalak, B.J. Dair, M.S. Capel, and E.L. Thomas, *Macromolecules*, **33**, 6502–6516 (2000).
[3] Y. Cohen, M. Brinkmann, and E.L. Thomas, *J. Chem. Phys.*, **114**, 984–992 (2001).
[4] K. Kawahara, R. Suzuki, and M. Tokita, *Macromol. Chem. Phys.*, **224**, 2300032 (2023).
[5] K. Osada, M. Koike, H. Tagawa, M. Tokita, and J. Watanabe, *Macromol. Chem. Phys.*, **205**, 1051–1057 (2004).
[6] M. Tokita, K. Tokunaga, S.I. Funaoka, K. Osada, and J. Watanabe, *Macromolecules*, **37**, 2527–2531 (2004).
[7] M. Tokita and J. Watanabe, *Polym. J.*, **38**, 611–638 (2006).
[8] S. Yagi, M. Oguro, and M. Tokita, *Macromol. Chem. Phys.*, **223**, 2100399 (2022).
[9] T. Murayama, E. Abe, and H. Saito, *Polymer*, **236**, 124343 (2021).
[10] K. Hagihara, Z. Li, M. Yamasaki, and Y. Kawamura, *Acta Mater.*, **163**, 226–239 (2019).
[11] D. Matsui, K. Morita, D. Terada, K.I. Ikeda, and S. Miura, *Mater. Trans.*, **63**, 1055–1064 (2022).
[12] N. Shimizu, T. Mori, N. Igarashi, H. Ohta, Y. Nagatani, T. Kosuge, and K. Ito, *J. Phys. Conf. Ser.*, **425**, 202008 (2013).
[13] J. Kuribayashi, R. Ishige, M. Hayashi, and M. Tokita, *Macromol. Chem. Phys.*, **221**, 2000042 (2020).
[14] S. Sakurai, S. Aida, S. Okamoto, K. Sakurai, and S. Nomura, *Macromolecules*, **36**, 1930–1939 (2003).
[15] N. Kasai and M. Kakudo, “X-Ray Diffraction by Macromolecules”, Springer Berlin Heidelberg, Berlin, Heidelberg (2005).

*tokita.m.aa@m.titech.ac.jp